ISSN: 2572-3243

Bitterman et al. J Musculoskelet Disord Treat 2018, 4:049
DOI: 10.23937/2572-3243.1510049
Volume 4 | Issue 2
Open Access

Journal of
Musculoskeletal Disorders and Treatment

ORIGINAL RESEARCH

Oral Ibuprofen Interferes with Cellular Healing Responses in a Murine Model of Achilles Tendinopathy

Adam Bitterman[1,2], Shuguang Gao[3], Sabah Rezvani[4], Jun Li[3], Katie J Sikes[5], John Sandy[1], Vincent Wang[4], Simon Lee[1], George Holmes[1], Johnny Lin[1] and Anna Plaas[1,3]*

[1]*Department of Orthopaedic Surgery, Rush University Medical Center, USA*

[2]*Department of Orthopaedic Surgery, Donald and Barbara Zucker School of Medicine at Hofstra/Northwell, USA*

[3]*Department of Internal Medicine (Rheumatology), Rush University Medical Center, USA*

[4]*Department of Biomedical Engineering, Virginia Tech, USA*

[5]*Department of Clinical Sciences, Colorado State University, USA*

***Corresponding author:** *Anna Plaas, PhD, Department of Orthopaedic Surgery and Department of Internal Medicine (Rheumatology), Rush University Medical Center, 1611 W Harrison Street, Chicago, IL 60612, USA, E-mail: aplaas@gmail.com*

Abstract

Background: The attempted healing of tendon after acute injury (overloading, partial tear or complete rupture) proceeds via the normal wound healing cascade involving hemostasis, inflammation, matrix synthesis and matrix remodeling. Depending on the degree of trauma and the nature of the post-injury milieu, a variable degree of healing and recovery of function occurs. Post-injury analgesia is often achieved with NSAIDs such as Ibuprofen, however there is increasing evidence that NSAID usage may interfere with the healing process. This study aimed to investigate the cellular mechanism by which IBU therapy might lead to a worsening of tendon pathology.

Methods: We have examined the effect of oral Ibuprofen, on Achilles tendon healing in a TGFb1-induced murine tendinopathy model. Dosing was started 3 days after initial injury (acute cellular response phase) and continued for 22 days or started at 9 days after injury (transition to matrix regeneration phase) and given for 16 days. Cellular changes in tendon and surrounding peritenon were assessed using Hematoxylin/Eosin, chondroid accumulation with Safranin O and anti-aggrecan immunohistochemistry, and neo-vessel formation with GSI Lectin histochemistry. Markers of inflammation included histochemical localization of hyaluronan, immunohistochemistry of heavy chain 1 and TNFα-stimulated glycoprotein-6 (TSG6). Cell responses were further examined by RT-qPCR of 84 NFκB target genes and 84 wound healing genes. Biomechanical properties of tendons were evaluated by tensile testing.

Results: At a clinically-relevant dosage, Ibuprofen prevented the process of remodeling/removal of the inflammatory matrix components, hyaluronan, HC1 and TSG6. Furthermore, the aberrant matrix remodeling was accompanied by activation at day 28 of genes (*Col1a2, Col5a3, Plat, Ccl12, Itga4, Stat3, Vegfa, Mif, Col4a1, Rhoa, Relb, F8, Cxcl9, Lta, Ltb, Ccl12, Cdkn1a, Ccl22, Sele, Cd80*), which were not activated at any time without the drug, and so appear most likely to be involved in the pathology. Of these, *Vegfa, Col4a1, F8, Cxcl9* and *Sele*, have been shown to play a role in vascular remodeling, consistent with the appearance at 25 days of vasculogenic cell groups in the peritenon and fat pad stroma surrounding the Achilles of the drug-dosed mice. Tensile stiffness ($p = 0.004$) and elastic modulus ($p = 0.012$) were both decreased (relative to age-matched uninjured and non-dosed mice) in mice dosed with Ibuprofen from day 3 to day 25, whether injured or not.

Conclusion: We conclude that the use of Ibuprofen for pain relief during inflammatory phases of tendinopathy, might interfere with the normal processes of extracellular matrix remodeling and cellular control of expression of inflammatory and wound healing genes. It is proposed that the known COX2-mediated anti-inflammatory effect of ibuprofen has detrimental effects on the turnover of a pro-inflammatory HA matrix produced in response to soft-tissue injury, thus preventing the switch to cellular responses associated with functional matrix remodeling and eventual healing.

Keywords

Tendinopathy, NSAID, Inflammation, Wound healing, Hyaluronan, Angiogenesis, Biomechanical properties

Citation: Bitterman A, Gao S, Rezvani S, Li J, Sikes KJ, et al. (2018) Oral Ibuprofen Interferes with Cellular Healing Responses in a Murine Model of Achilles Tendinopathy. J Musculoskelet Disord Treat 4:049. doi.org/10.23937/2572-3243.1510049

Accepted: May 19, 2018: **Published:** May 21, 2018

Abbreviations

TGF-β1: Transforming Growth Factor beta 1; IBU: Ibuprofen; ECM: Extracellular Matrix; UI: Uninjured; COV: Coefficient of Variation; NSAIDs: Non-Steroidal Anti-inflammatory Drugs; HA: Hyaluronan; HC1: Inter-alpha-trypsin Heavy Chain 1; EMT: Epithelial Mesenchymal Transition; IaI: Inter-alpha-trypsin Inhibitor

Introduction

The Achilles tendon is the largest tendon in the body. Its primary function involves push-off and maintaining the overall position of the tibia during gait. Tendinopathy of the Achilles is a major health care concern with specific focus to orthopaedic foot and ankle surgeons. It often presents as pain and swelling within the tendon proper, and has been found to be associated with obesity, hypertension, and steroid use [1], each of which have shown an end-organ effect of a decrease in local microvascularity. While this correlation is consistent with a role for hypoxia in the development of Achilles tendinopathy [2], effective therapies to alleviate symptoms remain limited. Current treatment protocols frequently include non-steroidal anti-inflammatory drugs (NSAIDs such as Ibuprofen) in combination with activity modification, rest, physical therapy and various bracing modalities. Surgical options do exist however they involve significant compliance during recovery and may lead to worsening morbidity related to wound complications or improper healing (reviewed in [3]). While NSAIDs provide short-term relief of pain through inhibition of cyclooxygenases-1 and -2, (and thereby inhibition of prostaglandin production), it is also well established that NSAIDs modulate multiple targets and can have multiple molecular effects apparently unrelated to cyclooxygenase inhibition [4]. These effects include binding to membrane transporters, such as hPEPT1 [5], enhancing microtubule formation in epithelial cells [6], modulation of cell membrane topography [7], inhibition of caspases [8] and induction of apoptosis [9]. NSAIDs have also been implicated in cardiac pathology [10] and there is mounting evidence that ibuprofen may also interfere with tendon repair [11-13].

Objectives

We aimed to describe the effect of IBU therapy on tendon pathological features in a murine model of tendinopathy, and to provide mechanistic details of the cellular responses involved.

Materials and Methods

Murine achilles tendinopathy model and ibuprofen administration

Unilateral tendinopathy was induced in the Achilles tendon of skeletally mature male C57Bl/6 mice by injections, on days 0 and 2, of 100 ng of active rhTGF-β1 (human recombinant, Peprotech, Inc., Rocky Hill, NJ) into the mid-portion of the tendon [2,14-16]. The injections were given between 2 pm - 4 pm and all euthanasia and tissue collections were between 9 am - 11 am. Mice had free access to food and drinking water and were allowed normal cage activity.

Ibuprofen (IBU) was administered orally as described by Ezell, et al. [17]. Briefly, a pediatric IBU oral suspension (20 mg/mL, CVS Pharmacy) was diluted with purified water to a final concentration of 1 mg/mL. Drinking bottles were wrapped in silver foil and the drug was renewed every 5 days. Drug was either initiated at 3 days after initial injury (acute cellular response phase) and administered for 22 days or initiated at 9 days after injury (matrix regeneration phase) and administered for 16 days. Average water consumption was ~3.8 mL (~3.8 mg IBU) per mouse per day. Experimental groups, outcome measures, and mouse numbers for each, are summarized in Supplementary Table 1. Mice were weighed before induction of tendinopathy and again before euthanasia, and no marked difference in average body weight was observed between experimental groups. All animal use was approved by the IACUC of Rush University.

QPCR Gene expression assays

Following euthanasia, Achilles tendons (including peritenon) were immediately isolated from all surrounding tissue, placed in RNA. Later and stored at -20 °C. RNA was isolated from each pool of tissue generated for each experimental group (Supplementary Table 1), as previously described [14]. Briefly, pooled tissue was fragmented under liquid nitrogen in a Bessman Tissue Pulverizer and extracted in 1 mL of Trizol by vortexing for 60 seconds. RNA purification was done with the RNeasy MiniKit (Qiagen, Cat #: 74104, Valencia, CA), and yields were between 300-500 ng RNA per tendon. RNA quality (A260:A280) was > 1.90 for all preparations, and 2 ug of each preparation was used for cDNA synthesis with the RT2 First Strand Kit (Qiagen). mRNA abundance for 84 NFκb target genes and 84 wound healing genes were determined using SYBR qt-PCR array plates (PAMM-121A, PAMM-225ZA Qiagen, Valencia, CA). Alphabetic gene listings are shown in Supplementary Table 2 and Supplementary Table 3. The reproducibility of the QPCR array assay was confirmed as described previously [3,18]. It should be noted that data for individual pools represents the average expression in 14-20 individual tendons (Supplementary Table 1). Changes in transcript abundance (ΔCt = Ct for transcript of interest minus Ct for the housekeeping gene, *B2m*) were used to calculate the fold change (2^-ΔΔCt) relative to un-injured levels for each experimental and control group. A 1-way ANOVA with Tukey's post-hoc tests was conducted using GraphPad Prism 7 (La Jolla, CA) on the ΔCt values to determine the significance ($p < 0.05$) of differences in the expression of genes. Specifically, 25 d post-injury data was compared to UI data and either E-IBU or L-IBU data.

Histology and immunohistochemistry

Ankle joints (n = 3 per experimental group) were processed as previously described [14,15]. Briefly, joints

were fixed in formaldehyde, decalcified in EDTA, processed, embedded in paraffin, and 5 µm thin sagittal sections cut through the entire joint. Sections (n = 36) from the mid-portion of each specimen, which included the Achilles-calcaneus insertion and the bursa were stained as follows: For histopathological evaluation of tissue responses to injury and drug treatment, section numbers 1,7,13,20,25,31 were stained with Hematoxylin/Eosin [14] and section numbers 2,14,21,26,32 were stained with Safranin-O (SafO) [15]. The remaining sections were used for immunohistochemistry: Briefly, sections (n = 6 per antibody) were deparaffinized and incubated overnight at 4 °C with the following probes: anti-TSG6 (5 ug/mL [19]), anti- Inter-alpha-trypsin Heavy Chain 1 (HC1) (1 ug/mL [20]) or aggrecan-DLS (1 ug/mL [15]), followed by biotinylated anti-rabbit IgG as secondary antibody. HA (hyaluronan) was localized with biotinylated HABP [18]. Neovascularization in the peritenon and the fat pad was assessed by immunochemistry with GSI Lectin (10 ug/mL; Vector Laboratories, Inc. Burlingame, CA 94010) [21]. All sections were counterstained with methyl green. Negative control staining is shown in Supplementary Figure 1.

Biomechanical testing

Tensile testing and analysis of mechanical properties were carried out as described by Wang, et al. [22]. Briefly, the Achilles/calcaneus complex was dissected from the surrounding tissues, followed by measurements of tendon width and thickness, from which cross-sectional was computed. The foot was potted in dental cement and the tendon-bone construct was mounted onto a materials testing system (MTS Insight 10, Eden Prairie, MN). Tensile testing (in a saline-filled chamber) consisted of preconditioning followed by a load to failure test at 0.05 mm/sec. 1-way ANOVA and Tukey's Multiple Comparison Tests were performed using JMP (SAS, Cary, NC) for statistical analysis of the data obtained from the 5 experimental groups listed in Supplementary Table 1.

Results

Histological evaluation of Achilles tendon pathology and ECM changes following TGFb1-induced injury and subsequent recovery

Low magnification SafO of the ankle joint (Supplementary Figure 2A) showed that by 3 d there was hy-

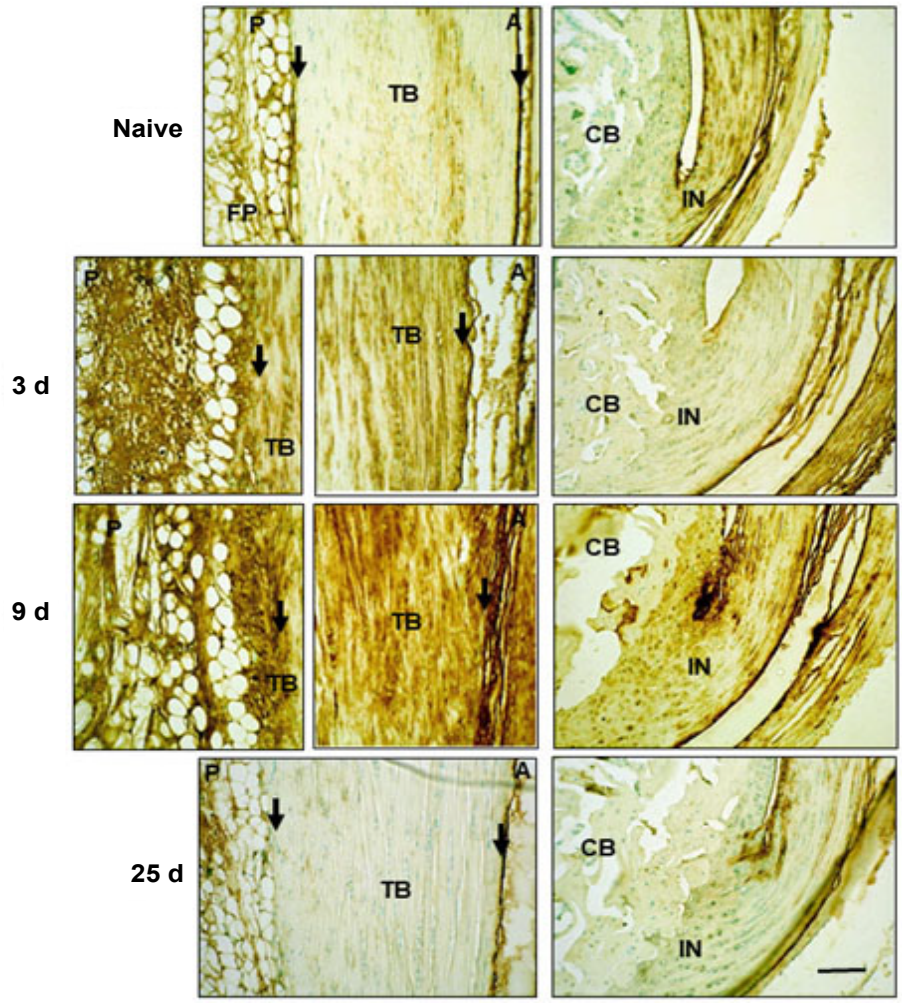

Figure 1: Histochemical localization of HA in Achilles tendon and surrounding tissues following TGFb1 induced injury.

Sections were treated and stained with HABP as described in the Methods. TB: Tendon Body; FP: Fat Pad; CB: Cancellous Bone; P: Posterior; A: Anterior; IN: Insertion site. Peritenon regions are indicated by black arrows and the space bar in the bottom panel = 100 µm.

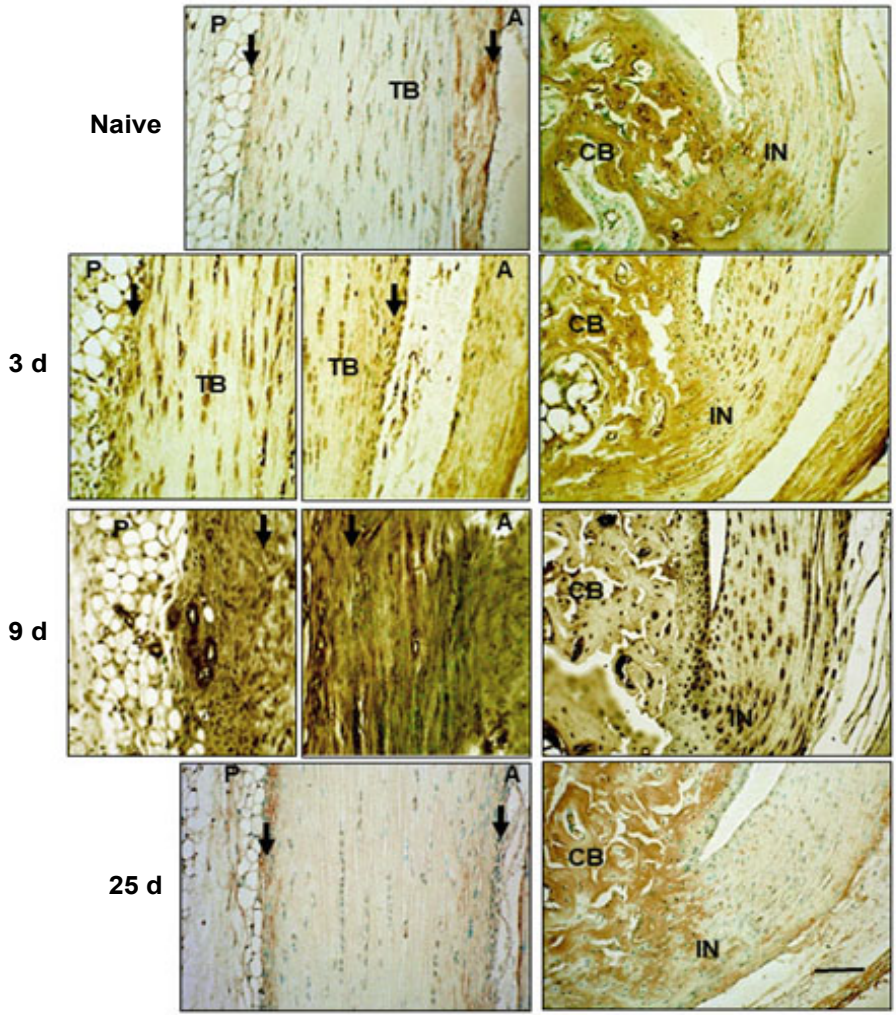

Figure 2: Immunohistochemical localization of HC1 in Achilles tendon and surrounding tissues.

Sections were stained with anti-HC1 antibodies following Proteinase K treatment for antigen retrieval, as described in the Methods. TB: Tendon Body; FP: Fat Pad; CB: Cancellous Bone; P: Posterior; A: Anterior; IN: Insertion site. Peritenon regions are indicated by black arrows, and the space bar in the bottom panel = 100 μm. The staining of the cancellous bone represents non-specific staining due to binding of the secondary antibody in proteinase K pretreated samples.

perplasia of both the anterior peritenon and fat pad and the posterior peritenon along with swelling of the tendon body. By 9 d, remodeling of the tendon ECM was evident as shown by chondroid deposition. At 25 d, there was evidence for reversal and repair as suggested by chondroid removal and the essentially normal appearance of both the peritenon and fat pad. The pattern of chondroid deposition in the model was confirmed by IHC localization of aggrecan-positive cells (Supplementary Figure 2B). Transient accumulation of neutrophils in vascularized regions of the fat pad were also observed in this acute phase response to the TGFb1 injury (Supplementary Figure 3).

To more closely define ECM changes in the inflammatory response to the TGFb1 injury, we performed IHC localization of components of the well-characterized inflammatory HA matrix [22-25], typically containing HA (Figure 1), HC1 (Figure 2) and TSG6, which transfers HC1 from bikunin onto HA [25] (Figure 3). HA staining increased between 3 d and 9 d, together with HC1 and TSG6, and this was evident in the tendon body, insertion sites, the peritenon and adipose stroma. By d 25 however, HA and HC1 reactivity was greatly diminished, indicating a clearance of this pro-inflammatory matrix most likely by resident phagocytic cells, including macrophages [27,28]. In contrast, TSG6 protein remained elevated in tendon cells, even at d 25 post-injury, however this did not appear to maintain a high level of HC1-HA matrix, presumably due to a lack of substrate HA or Inter-alpha-trypsin inhibitor (IaI), or inactivation of the transferase activity of the TSG6.

Time course of expression of wound healing and NFκb target genes in Achilles tendons following TGFb1-induced injury and during subsequent recovery

The expression of genes in Achilles tendons (including peritenon) from naïve mice and at 3 d, 9 d and 25 d after injection of TGFb1 were determined. For each array (Table 1 and Table 2), the genes are arranged alphabetically under each pathway group and the values show the fold-change in expression at each time point, relative to UI levels.

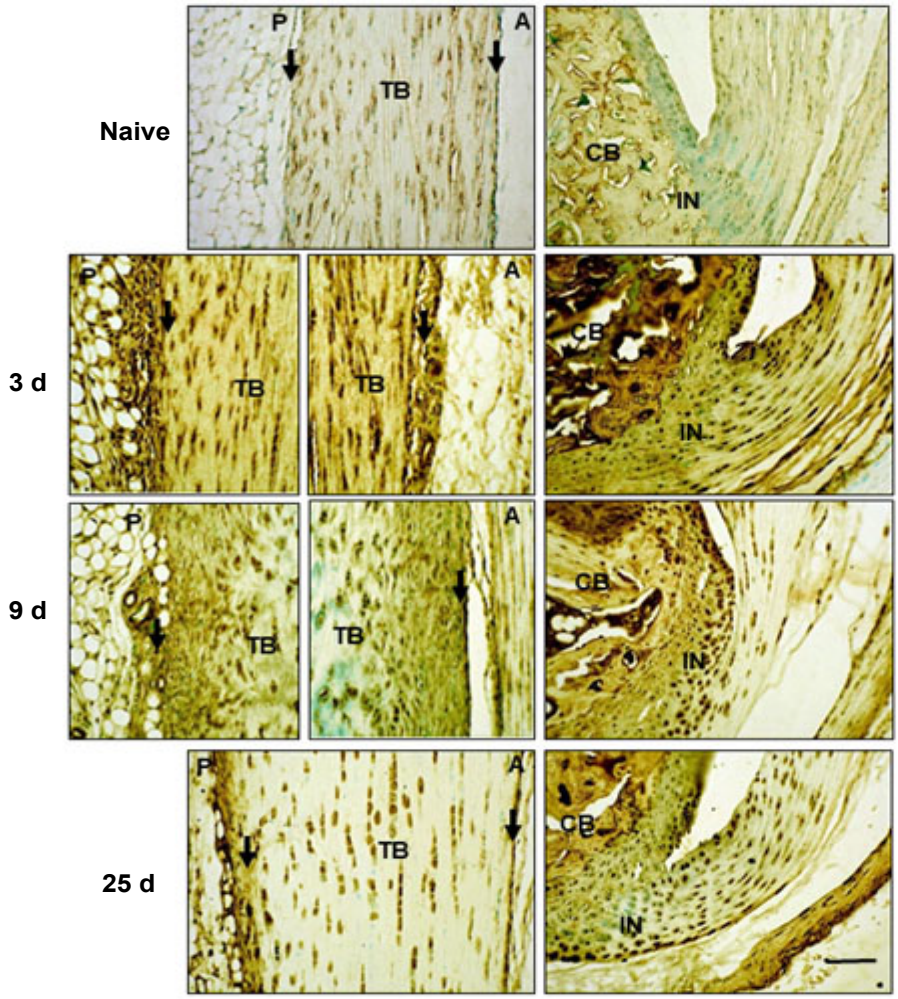

Figure 3: Immunohistochemical localization of TSG6 in Achilles tendon and surrounding tissues.

Sections were stained with anti-TSG6 antibody, as described in the Methods. TB: Tendon Body; FP: Fat Pad; CB: Cancellous Bone; P: Posterior; A: Anterior; IN: Insertion site. Peritenon regions are indicated by black arrows, and the space bar in the bottom panel = 100 μm.

Table 1: Fold Change expression (relative to UI) of Wound Healing genes after injection of TGF-β1.

Gene‡	Fold Change‡‡			p#
	3 d	9 d	28 d	
ECM Structure				
Col14a1	-	12.6	4.4	**
Col1a1	-	10.7	3	*
Col1a2	-2.4	2.2	-	
Col3a1	3.5	6.1	-	
Col4a1	-	2.7	-	
Col4a3	-4.5	-1.7	-	
Col5a1	5.6	10.1	-	
Col5a2	4.4	7.8	-	
Col5a3	4	3	-	
ECM Remodeling enzymes				
Ctsk	-2.2	7.1	3.8	***
Ctsl	-	2.1	1.6	
Mmp2	-	11.7	6	**
Mmp9	9.7	10.4	-	
Plat	3	4.6	1.5	
Plau	4.2	2.6	-	
Plaur	-4	6.7	1.6	
Plg	4.2	-1.6	-	
Serpine1	108.1	10.7	1.9	
Timp1	13.3	9.3	2.7	
Cell Adhesion molecules				
Cdh1	66.5	35.4	6.1	**
Itga1	-2.3	-	-	
Itga2	-4	-	-	
Itga3	-	1.9	-	
Itga4	2	2	-	
Itga5	6.8	4.4	1.7	
Itga6	-	-	-	
Itgav	2.3	2.1	1.5	
Itgb1	2	3.1	1.9	***
Itgb3	-	2	1.6	
Itgb5	-	1.7	1.6	**
Itgb6	-11.6	-2.6	-	
Cytoskeleton				
Acta2		1.5		
Actc1	-12.9	-1.5	-2	
Rac1	-1.4	-	-	
Rhoa	1.2	2.1	-	
Tagln	-2	-	-	
Growth factors & cytokines				
Angpt1	-1.7	2.7	2.1	*
Ccl12	-	2.5	-	
Ccl7	14.5	2.7	-	
Cd40lg	-3.1	2	-2	
Csf2	-	2.5	1.8	

Csf3	-	-1.7	-	
Ctgf	-1.6	-1.5	1.8	
Ctnnb1	1.9	4.1	2.1	
Cxcl11	-12.7	-2.2	-2	
Cxcl5	510.2	16.3	-3.8	
Egf	-2.6	1.7	-	
Egfr	-	2.6	-	
Fgf10	-11	-4	-2.8	*
Fgf2	-	1.7	1.7	
Fgf7	-1.7	-1.3	1.5	
Hbegf	6.7	3.3	-	**
Hgf	7.1	6.9	3.3	
Igf1	-	7.6	-	
Il10	2.2	6.6	-	*
Il6st	-1.1	1.6	2.4	
Mapk1	-	1.7	1.8	
Mapk3	-	3	3.1	*
Mif	3.5	2.8	-	
Pdgfa	-	2.1	-	
Pten	-	1.9	-	
Stat3	2.6	3.8	1.6	
Tgfb1	2.7	2.7	1.6	
Tgfbr3	-1.8		1.9	
Tnf	6	7.2	1.5	
Vegfa	-	-	-1.6	
Wisp1	8.7	7.8	-	

‡Genes are organized in functional groups.

A complete listing of all genes on the array plates is shown in Supplementary Table 2 and mRNA abundance values for each gene in the UI tendons is shown in Supplementary Table 4.

‡‡3 replicate tissue pools were analyzed for UI and 28 d groups and duplicate pools for 3 d and 9 d groups (see Table 1 for details).

#Statistical analyses was performed for comparison of UI and 28 d groups, with p values (*) = 0.05, (**) = 0.01, (***) = 0.001, (****) = 0.0001.

Genes for which expression was unaffected relative UI samples are marked with (-).

Wound healing pathway genes (Table 1) which were > 5-fold activated at 3 d included ECM structure genes (*Col5a1*), ECM remodeling factors (*Timp1, Mmp9*, *Serpine1*), cell adhesion proteins (*Itga5, Cdh1*), growth factors (*Hbegf*, *Hgf, Wisp1*) and chemokines (*Ccl7*, *Cxcl5*). NFκb target genes > 5-fold activated at 3 d (Table 2) included chemokines and cytokines (*Tnf*, *Ilr2*, *Cxcl1, Cxcl3*, *Il1b, Il6*), acute inflammatory response proteins (*Ptgs2, Tnfrsf1b*, *Myd88*), a stress factor (*Plau*), an NFκb signaling factor (*Rel*) and an apoptosis factor (*Nr4a2*). Of the 23 genes activated > 5-fold at 3 d, all but three (*Col5a1*, *Mmp9* and *Tnf*) were still activated at 9 d (Table 1 and Table 2) but returned close to naïve expression levels by 25 d, consistent with the histological changes indicating a resolution of the inflammatory wound healing response at that time (Figure 1, Figure 2 and Supplementary Figure 2). Notably, a different group of 21 genes (*Col14a1*, *Col1a1*, *Col3a1*, *Col5a2*, *Ctsk*, *Mmp2*, *Mmp9*, *Plaur*, *Igf1*, *Il10*, *Tnf*, *Ccl5*, *Cxcl10*, *Il12b*, *Il1rn*, *Ccr5*, *C4a*, *Bcl2a1a*, *Vcam1*, *Cd83*) were more highly expressed at 9 d than at 3 d and for 10 of these (*Col14a1*, *Col1a1*, *Mmp2*, *Igf1*,

Table 2: Fold Change expression (relative to UI) of Nfkb Target genes after injection of TGF-β1.

Gene‡	Fold Change‡‡			p#
	3 d	9 d	28 d	
Cytokines & Chemokines				
Ccl12	-	4	-	
Ccl22	-4.6	3.2	-	
Ccl5	-	18	-	
Csf3	-	3.6	-	
Cxcl1	28	15.9	2.5	
Cxcl10	3.1	8.6	-	
Cxcl3	136.7	7.5	4.6	
Cxcl9	-1.8	3.9	-	
Ifng	-	3.1	-	
Il12b	-	13.7	2.2	
Il15	-5.4	2.2	-	***
Il1b	108.1	42.9	17.4	
Il1rn	4.3	9.7	-	
Il4	-5.5	-5.9	-3.2	***
Il6	141.9	42.8	1.8	
Lta	-2.5	-	-2.8	**
Ltb	-	2.5	-	
Tnfsf10	-42.4	-	-	
Ccr5	4.9	5.9	-	
Il1r2	17.3	-	-2	
Il2ra	-19.2	-	-	
Acute inflammation				
C4a	-	5.7	5.2	****
F3	-7	-2.4	-	
F8	-2.6	3.9	-	
Stat3	-	2	-	
Agt	-10	-	-	
Myd88	17	7	2.5	**
Ptgs2	492.3	92.3	10.7	**
Sele	-	2	-	
Tnfrsf1b	6.4	2.7	2.3	**
Type I Interferon Responsive				
Cd80	-	2.1	-	
Cdkn1a	-1.9	2.4	-	
Cfb	-2.8	1.8	-	
Ncoa3	-8.2	-	-	
Irf1	-2.2	-	-	
NFκB Signaling				
Nfkb1	-2	-	-	
Nfkb2	-	2.5	2.6	****
Relb	2.3	4.6	-	
Cd40	2.1	2.8	-	
Rel	11	4.9	-	
Transcription factors				
Egr2	-	4.1	-	
Myc	2.6		-	
Trp53	-	3.7	-	
Stat5b	-2.1	-	-	
Anti-Apoptotic	-		-	
Akt1		2.9		
Bcl2a1a	-	5.3	-	
Birc3	-	4	3.9	**
Fas	-6	-	-	
Sod2	-5.1	-1.9	-	
Xiap	-3.5	-	-	
Apoptosis				

Birc2	-3.9	-	-	
Cd74	-	2	2	**
Egfr	-2.8	3.1		
Fasl	4.8	-	2.6	
Map2k6	-10.8	-	-	
Mitf	-19	-	-	
Mmp9	3.5	7.2	-	
Nqo1	-26.1	-	-	
Nr4a2	18.6	18.3	8.6	***
Vcam1	-	13.8	5.8	**
Stress Responses				
Ccnd1	-	2.9	-	
Plau	8.4	-	-	
Other Immune Response				
Cd83	-	7.4	3.2	*

‡Genes are organized in functional groups.

A complete listing of all genes on the array plates is shown in Supplementary Table 3 and mRNA abundance values for each gene in the UI tendons is shown in Supplementary Table 4.

‡‡3 replicate tissue pools were analyzed for UI and 28 d groups and duplicate pools for 3 d and 9 d groups (see Table 1 for details).

#Statistical analyses was performed for comparison of UI and 28 d groups, with p values (*) = 0.05, (**) = 0.01, (***) = 0.001, (****) = 0.0001.

Genes for which expression was unaffected relative UI samples are marked with (-).

Il10, *Ccl5*, *Il12b*, *C4a*, *Bcl2a1a*, *Vcam1*, *Cd83*) the initial activation was even delayed until 9 d, consistent with a primary role for these genes in the transition from acute inflammation (3 d) to tissue recovery (25 d). Thus, the initial increase in expression of *Col14a1*, *Col1a1*, *Col3a1*, *Col5a1*, *Col5a2* and *Igf1* at 9 d would be expected to promote repair of the collagenous and proteoglycan matrix respectively, and normalization of expression of these genes at 25 d indicates that the repair was largely complete, much as observed histologically (Figure 1, Figure 2 and Supplementary Figure 2). In contrast, seven genes (*Il1b*, *C4a*, *Ptgs2*, *Nr4a2*, *Vcam1*, *Mmp2* and *Cdh1*) remained greater than 5-fold activated at 25 d, suggesting that the initial inflammatory response, indicated by high expression of *Il1b* and *Ptgs2,* was not entirely resolved even at 25 d, also consistent with the high TSG6 protein at this time (Figure 3).

A consideration of established functions, suggests that at least some of the 23 genes activated > 5-fold on 3 d are apparently involved in development of the 9 d pathology (tissue swelling, chondroid deposition, inflammatory HA matrix deposition). For example, *Serpine1* and *Timp1* can be broadly considered as markers of fibrosis [28,29] whereas activation of *Cdh1 (*E-cadherin) suggests epithe-

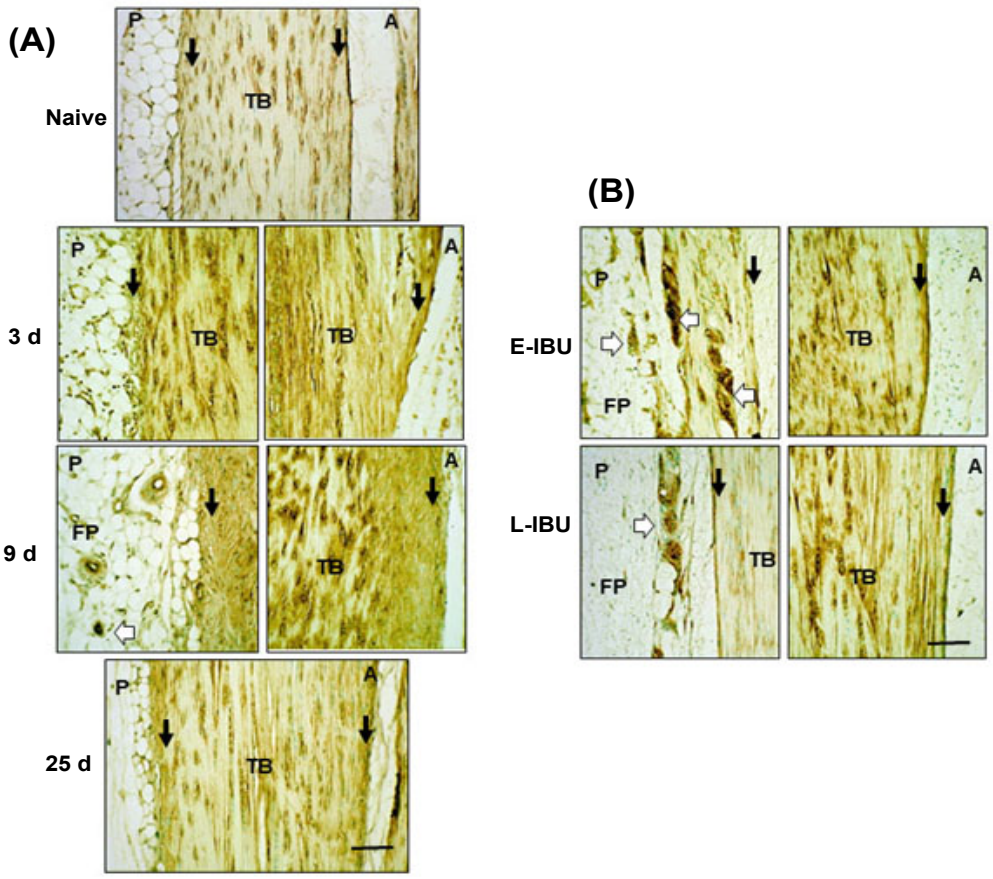

Figure 4: Histochemical Staining with GSI Lectin of the Achilles tendon and surrounding tissues following TGFb1 induced injury without (A) and with (B) IBU treatment.

Sections were treated and stained with GSI Lectin, as described in the Methods. TB: Tendon Body; FP: Fat Pad; P: Posterior; A: Anterior; Peritenon regions are indicated by black arrows and the space bar in the bottom panel = 100 μm. White arrows indicate the stained cell groups (indicative of vasculogenic mimicry) that accumulated in the fat pad stroma at 9 d post-injury and at 25 d in E IBU and L IBU groups.

lial-mesenchymal transitional (EMT) activity [31] in the peritenon. Furthermore, activated expression of *Il1b* and *Il1r2* indicates both a pro-inflammatory response to the injury and its local control by epithelial cells of the peritenon [32,33]. Activation of *Il6* (~142-fold) at 3 d is consistent with a broad effect of the injury on immune and non-immune cells with both, pro- and anti-inflammatory properties. In addition, the highly activated and coordinated expression of *Cxcl1* (~28-fold), *Cxcl3* (~137-fold) and *Cxcl5* (~510-fold) supports the occurrence of the pro-inflammatory response that has been reported after IL1β treatment of MSCs [34].

The expression of other genes (*Il15*, *Il4*, *Tnfsf10*, *Il-2ra*, *F3*, *Agt*, *Ncoa3*, *Fas*, *Sod2*, *Map2k6*, *Mitf*, *Nqo1*, *Itgb6*, *Actc1*, *Cxcl11*, *and Fgf10*) was inhibited greater than 5-fold at 3 d and all were essentially normalized by 25 d. A putative function for these genes in the injured tendon is not obvious, however in two cases where the genes have been shown to be protective (*Il4* [35] and *Sod2* [36]) the inhibition of expression would be expected to enhance the general inflammatory response.

Histological evaluation following TGFb1-induced injury and recovery in the presence of Ibuprofen

When compared to no drug, E-IBU had marked effects on the histological appearance of tendon and peritenon at 25 d. Tendons in dosed mice retained elevated levels of chondroid in the tendon body (Supplementary Figure 2A and Supplementary Figure 2B), indicating that E-IBU interfered with reparative removal of the accumulated post-injury ECM. Most notable however was the increased abundance of blood vessels in the adjacent fat pad (Supplementary Figure 3A) in both E-IBU and L-IBU groups at 25 d. The increased angiogenic response of fat pad stromal cells was confirmed by GSI lectin histochemistry (Figure 4), which has been used to assess formation of new blood vessel at sites of injury [3]. Without IBU dosing (Figure 4A) a minor and transient increase in small vessels was seen in the fat pad (white arrows) at 9 d, but no such structures were detectable at 25 d. By comparison, multiple groups of strongly GSI-positive cells were seen in the fat pads of both E-IBU and L-IBU groups (Figure 4B, white arrows). However, since the GSI-positive cells had not formed tubular structures, as expected of neo-vessels, they may represent either precursor neo-vessels, or partially differentiated multi-potent adipose-derived stromal cells, which can exhibit the 'vascular mimicry' which often accompanies epithelial-mesenchymal transition [37].

Additional histological differences between IBU-dosed and non-dosed specimens were seen after staining for HA and HC1 (Figure 5A and Figure 5B, respectively). In the non-dosed samples, HA and HC1 reactivity had been largely restored to low pre-injury levels by 25 d. This is likely through clearance of the pro-inflammatory matrix by resident phagocytic cells, including tissue macrophages [27], However, in both E-IBU and L-IBU groups, HA (Figure 5A) and HC1 (Figure 5B) staining remained elevated in the tendon body and throughout the peritenon, indicating that the drug dosing impaired or delayed the clearance of this pro-inflammatory matrix, and therefore prolonged inflammation and ECM remodeling by resident cells.

Effect of Ibuprofen dosing on expression of wound healing and NFκb target genes in Achilles tendons

At the histological level, IBU dosing resulted in in-

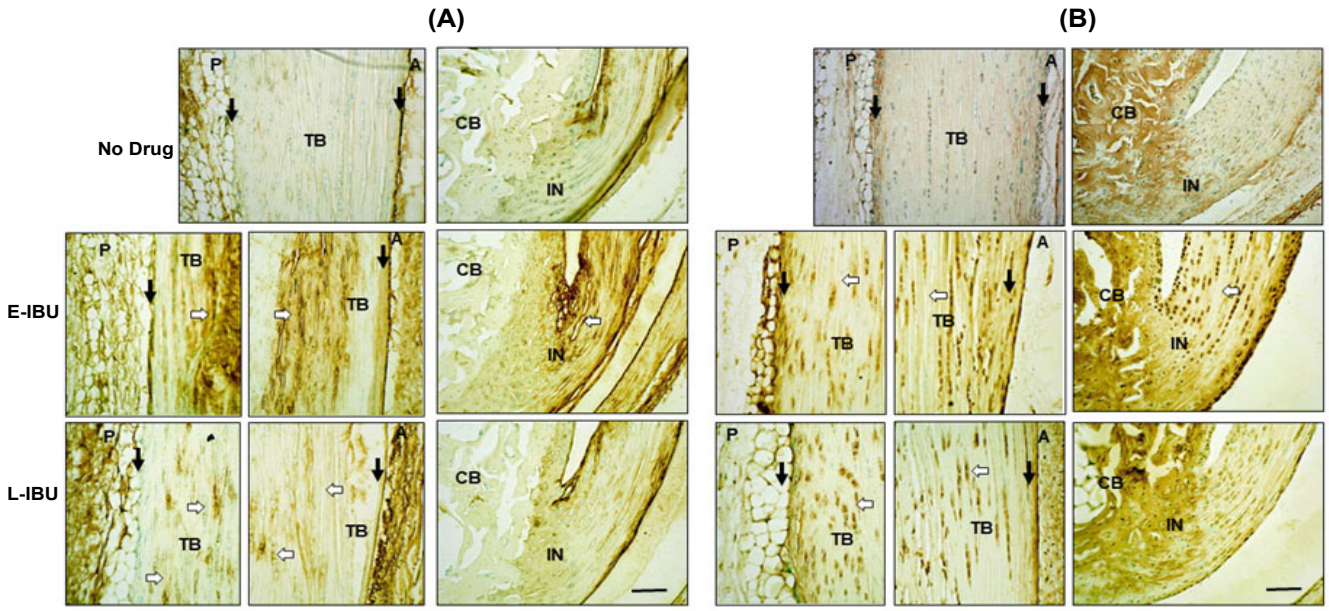

Figure 5: Accumulation of HA (A) and HC1 (B) in the tendon body and the peritenon at 25 d with IBU treatment.

Sections were stained as described in the Methods. TB: Tendon Body; CB: Calcaneus; IN: Insertion; P: Posterior; A: Anterior; Peritenon regions are indicated by black arrows and the space bar in the bottom panel = 100 μm. White arrows highlight ECM regions of the tendon body with persistent HA accumulation after IBU treatment (A), and persistence of HC1 positive tendon and at 25 d in E-IBU and L-IBU groups (B).

Table 3: Fold Change expression in Wound Healing and Nfkb Target Genes following Oral E-IBU and L-IBU dosing.

	Wound Healing		Nfkb Targets		
	Fold Change#		Fold Change#		
Gene‡	E-IBU	L-IBU	Gene‡	E-IBU	L-IBU
Cxcl5	28.4*	3.49*	*Il6*	7.84*	3.17
Col3a1	10.02*	2.27*	*Il1rn*	6.81*	3.92*
Mmp9	7.34*	45.01*	*Cxcl3*	6.11*	2.56
Col5a1	6.9*	4.32*	*Ptgs2*	5.95*	4.07*
Wisp1	5.69*	1.45	*Ccl5*	5.84*	3.41*
Col1a1	5.16*	1.39	*Cxcl10*	5.58*	2.73*
Col5a2	4.99*	3.68*	*Relb*	4.33*	2.35
Serpine1	4.72*	1.66	*F8*	4.1*	1.69
Timp1	3.91*	1.29	*Rel*	4.09*	2.01
Col1a2	3.83*	1.07	*Cxcl9*	3.78*	1.32
Col5a3	3.44*	1.66	*Lta*	3.46*	3.54
Cdh1	3.37*	-1.31	*Il12b*	3.26*	2*
Plat	3.19*	1.58	*Ltb*	3.23*	2.08
Ccl12	3.17*	1.15	*Ccr5*	3.2*	2.92*
Hgf	3.05*	1.44	*Ccl12*	2.92*	1.76
Itga4	3.01*	1.11	*Bcl2a1a*	2.83*	1.53
Stat3	2.75*	2.27	*Cdkn1a*	2.46*	1.8
Itga5	2.61*	1.16	*Ccl22*	2.34*	-1.09
Vegfa	2.49*	1.99	*Selp*	2.27*	2.98*
Ctsk	2.47*	1.8	*Tnf*	2.21*	1.32
Mif	2.22*	1.53	*Rela*	2.07*	1.98*
Col4a1	1.96*	1.27	*Sele*	2.06*	1.54
Rhoa	1.62*	1.65*	*Gadd45b*	1.98*	1.21
Cd40lg	1.11	3.99*	*Cd80*	1.84*	1.59*
Plg	-3.80*	-1.98	*Il1b*	1.76*	-2.7
			Nfkbia	1.64*	1.51*
			Ifng	1.11	2.47
			Csf3	1.07	4.25*

‡Genes are organized from highest to lowest fold activation; #Statistical analyses was performed for comparison with 25 d No Drug groups and *indicates $p < 0.05$.

creased levels of chondroid and HA/HC1 in the tendon as well as an apparent attempt at neovascularization of the fat pad stroma. Taken together, this suggested that the drug interfered with the capacity of cells to modulate inflammation associated pathways and to achieve clearance via remodeling of the post-injury generated ECM. To provide mechanistic insight we compared expression levels of Wound healing and NFκb target genes in tendons from IBU-dosed and non-dosed mice (Table 3). This analysis revealed that E-IBU resulted in a higher ($p < 0.05$) expression (relative to 25 d no drug), for 26 NFκb target genes and 24 wound healing genes, whereas L-IBU enhanced expression of only 11 and 6 genes respectively. This suggested that for most genes the drug-enhanced expression seen at 25 d was dependent on IBU administration starting in the acute inflammatory post-injury period (at 3 d). Since the relatively low expression at 25 d without IBU (Table 1 and Table 2) followed normalization from stimulated levels at 3 d and 9 d, the elevated levels at 25 d (relative to no dosing) would be consistent with a drug-mediated inhibition in the normalization process. If the apparent loss of clearing capacity with IBU dosing (i.e. accumulated chondroid, vascular adipose, GSI-positive cells and HA/HC1 matrix) results from the enhanced expression of genes (Table 3), this implicates up to 50 genes in the IBU-induced pathology. Of the 50 genes, 25 were activated by injury (relative to naïve) at 3 d and/or 9 d without drug (Table 1 and Table 2) and were also enhanced (relative to no drug) at 25 d by IBU dosing.

Genes that were not activated at any time in the no drug group, but enhanced by E-IBU appear most likely to have been responsible for the IBU-induced changes in cell responses and downstream pathology. Notably all of those have been reported to play a role in vascular remodeling (*Vegfa* [38], *Col4a1* [39], *F8* [40], *Cxcl9* [41], *Sele* [42]) consistent with the appearance at 25 d of vasculogenic cell groups in the peritenon and fat pad of the IBU-dosed mice.

It is worth noting that those genes where expression was inhibited (> 5-fold), rather than activated, at 3 d were essentially normalized by 25 d with no drug, and were not markedly affected by IBU dosing.

Notably, it was shown that IBU dosing of naïve mice for 22 days caused a 25-30% loss in stiffness and elastic modulus, suggesting that a low-level of PGE2-mediated inflammation is essential for normal homeostatic maintenance of tendon mechanics. However, IBU dosing also activated genes such as u-PAR (*Plaur*) which has been linked to tendon healing [43], *Itga5* and *RhoA* which have been linked to repair [44,45] and *Cd40lg* associated with inflammation control [46]. It is unknown how activation of these genes might lead to the observed loss of stiffness or elastic modulus in such tendons (Figure 6 and Supplementary Figure 4).

Effect of Ibuprofen dosing on biomechanical properties of Achilles tendons

Tensile stiffness ($p = 0.004$) and elastic modulus ($p = 0.012$) were both decreased (relative to age-matched uninjured and non-dosed mice) in mice dosed with IBU from 3 d to 25 d, whether injured (E-IBU) or not (UI-IBU) (Figure 6). This effect of IBU appears to be independent of the changes in wound healing and NFκb gene expression in injured samples (Table 3) since those changes required TGFb1 injection. No statistically significant differences were noted among the experimental groups with regard to cross-sectional area ($p = 0.56$), maximum load ($p = 0.90$), or maximum stress ($p = 0.89$). Additionally, no statistically significant differences were found for displacement at maximum force ($p = 0.09$) and strain at maximum stress ($p = 0.10$) (Supplementary Figure 4), although a statistical trend towards increases in these parameters with injury (with and without IBU) may contribute to the significant changes in stiffness and elastic modulus, respectively. Notably, the coefficient of variation (COV) for both geometric and mechanical properties was generally lowest for the UI-IBU group, while the COV of the E-IBU group was consistently high-

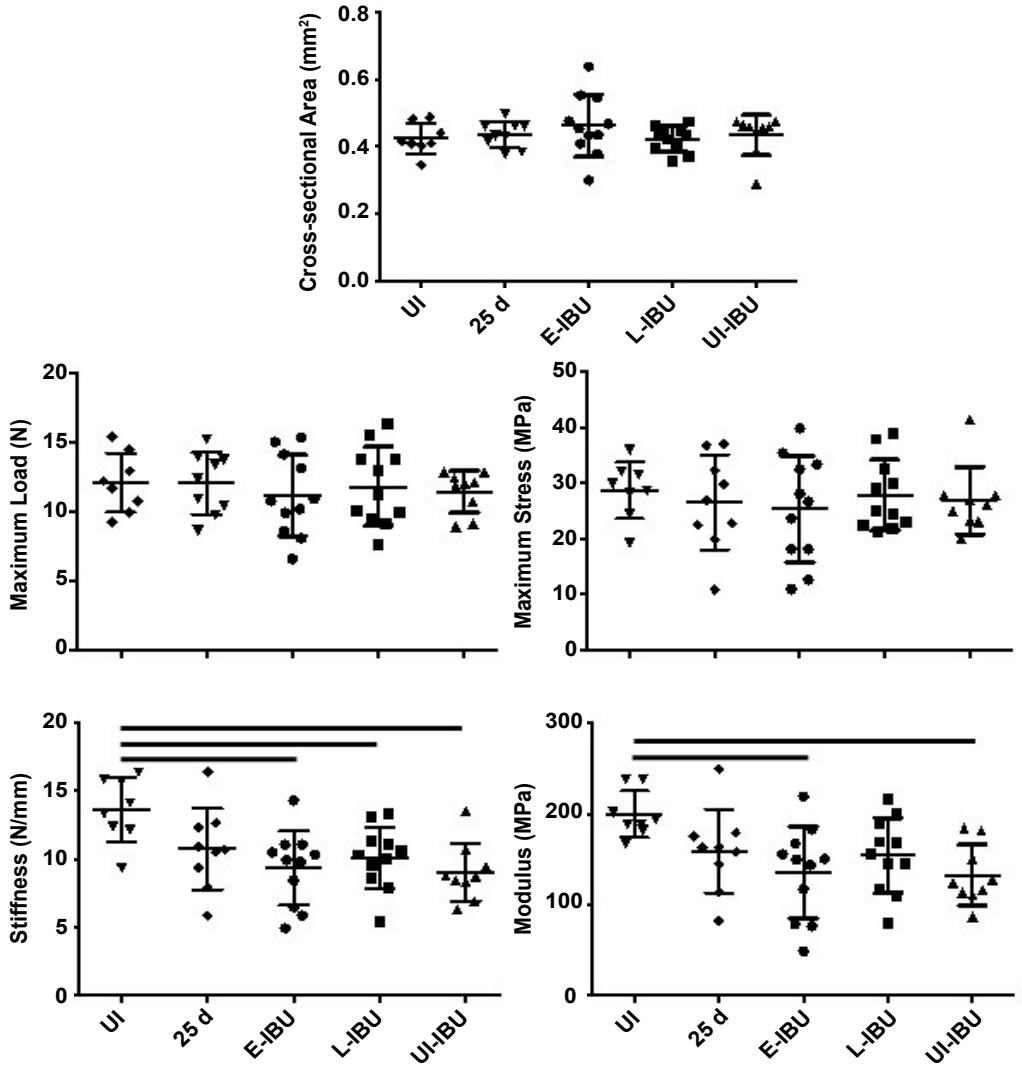

Figure 6: Effect of IBU administration on Achilles tendon mechanical properties.

The scatter plots show data for individual tendons in each group. For each group, horizontal lines denote mean ± one standard deviation. Horizontal lines above the plots denote statistically significant differences between groups.

er than that of the L-IBU group, particularly for material (in comparison to structural) properties.

Discussion

This study was motivated by the question of how dosing with NSAIDs such as IBU for pain relief, might influence the pathogenesis of tendinopathies [11-13]. For this purpose we studied the histopathological, biochemical responses and biomechanics of the Achilles tendon in a non-surgical model of tendinopathy in mice. Using such outcome measures, a detailed characterizing of phases of acute post-injury responses (1-2 weeks) followed by a recovery and repair period (2-4 weeks) has been reported [3,14,15].

The data obtained in this study reveals that IBU dosing, especially when started during the acute injury response period, prevents the restoration of ECM composition and re-establishment of pre-injury inflammation and wound healing gene expression levels. Regarding the mechanism of this effect, the analysis indicates that enhancement of expression of one or more of the genes described in Table 3 might be responsible. The most extreme activating effects of IBU on gene expression were for inflammatory mediators and ECM turnover components, including *Cxcl5* (28-fold higher than without IBU at 25 d), *Col3a1* (10-fold), *Il6* (7.8-fold), *Mmp9* (7.3-fold), *Col5a1* (6.9-fold), *Cxcl3* (6.1-fold) and *Ptgs2* (5.9-fold).

At the histological level, the finding that IBU prevents the clearance of the HA inflammatory matrix indicates that it interferes with the phagocytic activity of tendon cells functioning as M2 tissue macrophages [47,48]. An expected downstream effect of persistent inflammatory activity at the 'wound site" would be the deposition of 'scar' collagens such as collagen types III and V, the expression of which was in fact found to be markedly activated by E-IBU dosing (Table 1). Although we were not able to detect extensive scar tissue deposition in the tendon body, either histologically or geometrically over the experimental time period used, it remains to be determined if the maintenance of IBU-treated tendinopathic mice, either at cage or treadmill activity [14], would generate pathological scarring in the tendon

body and surrounding tissue. In the same context, 'angiogenic' stromal cell clusters in the peritenon and fat pad (Supplementary Figure 3) could progress to aberrant vascularization that has been reported in impaired wound healing [37] and in the stroma of rapidly growing tumors [49].

Whereas histologic analyses showed marked effects of IBU on tendon cell and ECM morphology at 25 d post-injury (Figures 4 and 5) biomechanical deficiencies were noted only for stiffness ($p = 0.004$) and elastic modulus ($p = 0.012$) for these tendons. This reflects sub-failure mechanical compromise caused here by IBU dosing both with and without TGF-β1 injury. In contrast, the absence of an effect of injury (with or without IBU) on maximum load, maximum stress and cross-sectional area shows that none of these treatments caused biomechanical changes typically associated with severe injury and rupture. Most notably, it was shown that IBU dosing of naïve mice for 22 days caused a 25-30% loss in stiffness and elastic modulus, which may be due to trended increases in displacement at maximum force ($p = 0.09$) and strain at maximum stress ($p = 0.10$) (Supplementary Figure 4). Taken together with increased expression of collagen types III, V, and IV, this data suggests the presence of an immature (un-crosslinked) and non-remodeled collagen matrix which contributes to larger strains, and decreased elastic modulus, similar to the use of glucocorticoids for tendon injury [50]. Further studies are warranted to confirm this phenomenon. In addition there was a consistent, general trend of increased spread (COV) in the E-IBU group for most parameters (Figure 6). We interpret this trend as biologically significant, consistent with the more marked effects of E-IBU than L-IBU on the gene expression profile (Table 3).

The current work supports the reported findings of deleterious effects of NSAIDs in the treatment of tendinopathies [11-13], but appears to conflict with the finding [51,52] that 7 days of oral IBU in patients with chronic Achilles tendinopathy produced no detectable changes in expression of COL1A1, TGF-β and PTGS2 in affected tendon tissue. The non-effect in the human studies however could be attributable to the short dosing period, chronic end-stage tendinopathy was studied and the dose (22.5 mg/kg/day) was low compared to the present model study (133 mg/kg/day). In addition, it may be relevant that a HA-HC-TSG6 inflammatory matrix and extensive scarring is found in the ligaments of DSLD affected horses [53] which are typically provided NSAIDs such as Phenylbutazone or Flunixin meglumine for pain relief (Brounts, S, personal communication).

To place the current findings in a broader clinical context, it appears useful to consider them in relation to the so-called continuum model [54,55], which predicts that treatment might be optimized (quote) "by tailoring interventions to the stage of pathology and targeting the primary driver (cell activation)". Indeed, the present study has provided support for the use of stage-specific treatments and has also generated novel information on the molecular aspects of the "cell activation" processes likely to be involved in different phases of the human pathology. The high animal to animal reproducibility of gene expression and histological changes in the model reported previously [3,14-16] and in the present study, revealed the existence of three phases, an initial inflammation (day 3), transition to a reparative phase (at day 9) and successful repair (by day 25) (see Results for details). In support of the importance of staged treatment, the start of IBU at day 3 resulted in poor repair at 25 days and over-expression of 50 target genes, whereas the start of IBU at 9 days enhanced repair and increased the expression of only 17 genes. Most notably, staged treatment also showed that early IBU dosing activated some genes unaffected by the TGFb1-injury itself and interestingly these have all been implicated in vascular remodeling (see Results for details), a feature of chronic tendinopathic tissue sections.

Conclusion

Our study with a non-surgically induced murine model of tendinopathy, showed that the use of Ibuprofen for pain relief during inflammatory phases of tendinopathy, might interfere with the normal processes of extracellular matrix remodeling and cellular control of expression of inflammatory and wound healing genes. In addition, the turnover of the post-injury inflammatory HA matrix was impaired, which may contribute to causing impaired cellular healing responses.

Limitations

Although we were not able, using the current experimental design, to detect extensive scar tissue deposition in the tendon body or surrounding tissues, either histologically or biomechanically, it remains to be determined if more prolonged maintenance of IBU-treated tendinopathic mice, either at cage or treadmill activity would lead to such degeneration and eventual rupture of the tendon itself. Furthermore, to what extent the results obtained here can inform clinical decisions will require analysis of human post-injury tendons using the molecular probes we have described. If tissues from human tendon injury patients on anti-inflammatory medication become available, it will be interesting to determine whether the analgesic benefits are accompanied by unacceptable levels of pro-inflammatory matrix accumulation and pro-inflammatory macrophage polarization.

Acknowledgments

Funding was provided by the Rush Arthritis Institute (AB, AP), Katz/Rubschlager Endowment for OA Research (AP) and NIH (AR 63144) (VMW SR, JL, and KJS). We thanks Dr. Sabrina Brounts, U WI for helpful discussions

regarding drug applications for pain management in DLSD affected horses.

Sources of Support

National Institute of Health (NIAMS); Rush Arthritis Institute (RUMC).

Statement of Equal Authors' Contribution

Adam Bitterman: Study design, animal model experimentation, data analyses, manuscript preparation.

Shuguang Gao: Gene expression assays, data analyses.

Sabah Rezvani: Biomechanical testing, data analyses.

Jun Li: Animal model experimentation, histology methods.

Katie J Sikes: Animal model experimentation, gene expression data statistical analyses, manuscript preparation.

John Sandy: Study design, manuscript preparation.

Vincent Wang: Study design, manuscript preparation.

Simon Lee: Study design.

George Holmes: Study design.

Johnny Lin: Study design.

Anna Plaas: Study design, animal model experimentation, data analyses, immunohistochemical analyses, manuscript preparation.

References

1. Holmes GB and J Lin (2006) Etiologic factors associated with symptomatic achilles tendinopathy. Foot Ankle Int 27: 952-959.
2. Sayegh ET, Sandy JD, Virk MS, Romeo AA, Wysocki RW, et al. (2015) Recent scientific advances towards the development of tendon healing strategies. Curr Tissue Eng 4: 128-143.
3. Sikes KJ, Li J, Gao SG, Shen Q, Sandy JD, et al. (2018) TGF-b1 or Hypoxia enhance glucose metabolism and lactate production via HIF1A signaling in tendon cells. Connect Tissue Res.
4. Dwivedi AK, Gurjar V, Kumar S, Singh N (2015) Molecular basis for nonspecificity of nonsteroidal anti-inflammatory drugs (NSAIDs). Drug Discov Today 20: 863-873.
5. Omkvist DH, B Brodin, CU Nielsen (2010) Ibuprofen is a non-competitive inhibitor of the peptide transporter hPEPT1 (SLC15A1): Possible interactions between hPEPT1 substrates and ibuprofen. Br J Pharmacol 161: 1793-1805.
6. Rymut SM, Kampman CM, Corey DA, Endres T, Cotton CU, et al. (2016) Ibuprofen regulation of microtubule dynamics in cystic fibrosis epithelial cells. Am J Physiol Lung Cell Mol Physiol 311: 317-327.
7. Boggara MB, M Mihailescu, R Krishnamoorti (2012) Structural association of nonsteroidal anti-inflammatory drugs with lipid membranes. J Am Chem Soc 134: 19669-19676.
8. Smith CE, Soti S, Jones TA, Nakagawa A, Xue D, et al. (2017) Non-steroidal anti-inflammatory drugs are caspase inhibitors. Cell Chem Biol 24: 281-292.
9. Todo M, Horinaka M, Tomosugi M, Tanaka R, Ikawa H, et al. (2013) Ibuprofen enhances TRAIL-induced apoptosis through DR5 upregulation. Oncol Rep 30: 2379-2384.
10. Arfè Andrea, Scotti Lorenza, Varas-Lorenzo Cristina, Nicotra Federica, Zambon Antonella, et al. (2016) Non-steroidal anti-inflammatory drugs and risk of heart failure in four European countries: Nested case-control study. BMJ 354: 4857.
11. Virchenko O, B Skoglund, P Aspenberg (2004) Parecoxib impairs early tendon repair but improves later remodeling. Am J Sports Med 32: 1743-1747.
12. Hammerman M, Blomgran P, Ramstedt S, Aspenberg P (2015) COX-2 inhibition impairs mechanical stimulation of early tendon healing in rats by reducing the response to microdamage. J Appl Physiol (1985) 119: 534-540.
13. Connizzo BK, Yannascoli SM, Tucker JJ, Caro AC, Riggin CN, et al. (2014) The detrimental effects of systemic Ibuprofen delivery on tendon healing are time-dependent. Clin Orthop Relat Res 472: 2433-2439.
14. Trella KJ, Li J, Stylianou E, Wang VM, Frank JM, et al. (2017) Genome-wide analysis identifies differential promoter methylation of Leprel2, Foxf1, Mmp25, Igfbp6, and Peg12 in murine tendinopathy. J Orthop Res 35: 947-955.
15. Bell R, Li J, Gorski DJ, Bartels AK, Shewman EF, et al. (2013) Controlled treadmill exercise eliminates chondroid deposits and restores tensile properties in a new murine tendinopathy model. J Biomech 46: 498-505.
16. Bell R, Li J, Shewman EF, Galante JO, Cole BJ, et al. (2013) ADAMTS5 is required for biomechanically-stimulated healing of murine tendinopathy. J Orthop Res 31: 1540-1548.
17. Ezell PC, Papa L, Lawson GW (2012) Palatability and treatment efficacy of various ibuprofen formulations in C57BL/6 mice with ulcerative dermatitis. J Am Assoc Lab Anim Sci 51: 609-615.
18. Chan DD, Xiao WF, Li J, de la Motte CA, Sandy JD, et al. (2015) Deficiency of hyaluronan synthase 1 (Has1) results in chronic joint inflammation and widespread intra-articular fibrosis in a murine model of knee joint cartilage damage. Osteoarthritis Cartilage 23: 1879-1889.
19. Mahoney DJ, Mikecz K, Ali T, Mabilleau G, Benayahu D, et al. (2008) TSG-6 regulates bone remodeling through inhibition of osteoblastogenesis and osteoclast activation. J Biol Chem 283: 25952-25962.
20. Yoshihara Y, Plaas A, Osborn B, Margulis A, Nelson F, et al. (2008) Superficial zone chondrocytes in normal and osteoarthritic human articular cartilages synthesize novel truncated forms of inter-alpha-trypsin inhibitor heavy chains which are attached to a chondroitin sulfate proteoglycan other than bikunin. Osteoarthritis Cartilage 16: 1343-1355.
21. Davidson YS, Clague JE, Horan MA, Pendleton N (1999) The effect of aging on skeletal muscle capillarization in a murine model. J Gerontol A Biol Sci Med Sci 54: 448-451.
22. Wang VM, Bell RM, Thakore R, Eyre DR, Galante JO, et al., (2012) Murine tendon function is adversely affected by aggrecan accumulation due to the knockout of ADAMTS5. J Orthop Res 30: 620-626.
23. Day AJ, CA de la Motte (2005) Hyaluronan cross-linking: A protective mechanism in inflammation? Trends Immunol 26: 637-643.
24. Petrey AC, CA de la Motte (2014) Hyaluronan, a crucial

regulator of inflammation. Front Immunol 5: 101.

25. Petrey AC, CA de la Motte (2016) Thrombin cleavage of Inter-α-inhibitor heavy chain 1 regulates leukocyte binding to an inflammatory hyaluronan matrix. J Biol Chem 291: 24324-24334.

26. Milner CM, AJ Day (2003) TSG-6: A multifunctional protein associated with inflammation. J Cell Sci 116: 1863-1873.

27. Majors AK, Austin RC, de la Motte CA, Pyeritz RE, Hascall VC, et al. (2003) Endoplasmic reticulum stress induces hyaluronan deposition and leukocyte adhesion. J Biol Chem 278: 47223-47231.

28. de la Motte CA, Hascall VC, Drazba J, Bandyopadhyay SK, Strong SA (2003) Mononuclear leukocytes bind to specific hyaluronan structures on colon mucosal smooth muscle cells treated with polyinosinic acid: polycytidylic acid: inter-alpha-trypsin inhibitor is crucial to structure and function. Am J Pathol 163: 121-133.

29. Yamanaka Y, Gingery A, Oki G, Yang TH, Zhao C, et al. (2018) Blocking fibrotic signaling in fibroblasts from patients with carpal tunnel syndrome. J Cell Physiol 233: 2067-2074.

30. Takawale A, Zhang P, Patel VB, Wang X, Oudit G, et al. (2017) Tissue inhibitor of Matrix Metalloproteinase-1 promotes Myocardial Fibrosis by mediating CD63-Integrin β1 interaction. Hypertension 69: 1092-1103.

31. van Roy F, G Berx, (2008) The cell-cell adhesion molecule E-cadherin. Cell Mol Life Sci 65: 3756-3788.

32. Bellehumeur C, Blanchet J, Fontaine JY, Bourcier N, Akoum A (2009) Interleukin 1 regulates its own receptors in human endometrial cells via distinct mechanisms. Hum Reprod 24: 2193-2204.

33. Stecco C, Cappellari A, Macchi V, Porzionato A, Morra A, et al. (2014) The paratendineous tissues: An anatomical study of their role in the pathogenesis of tendinopathy. Surg Radiol Anat 36: 561-572.

34. Carrero R, Cerrada I, Lledó E, Dopazo J, García-García F, et al. (2012) IL1β induces mesenchymal stem cells migration and leucocyte chemotaxis through NF-κB. Stem Cell Rev 8: 905-916.

35. McKelvey R, Berta T, Old E, Ji RR, Fitzgerald M (2015) Neuropathic pain is constitutively suppressed in early life by anti-inflammatory neuroimmune regulation. J Neurosci 35: 457-466.

36. Jiang D, Gao P, Lin H, Geng H (2016) Curcumin improves tendon healing in rats: A histological, biochemical, and functional evaluation. Connect Tissue Res 57: 20-27.

37. Liu Q, Qiao L, Liang N, Xie J, Zhang J, et al. (2016) The relationship between vasculogenic mimicry and epithelial-mesenchymal transitions. J Cell Mol Med 20: 1761-1769.

38. Pufe T, Petersen W, Tillmann B, Mentlein R (2001) The angiogenic peptide vascular endothelial growth factor is expressed in foetal and ruptured tendons. Virchows Arch 439: 579-585.

39. Rhodes CJ, Im H, Cao A, Hennigs JK, Wang L, et al. (2015) RNA sequencing analysis detection of a novel pathway of endothelial dysfunction in pulmonary arterial hypertension. Am J Respir Crit Care Med 192: 356-366.

40. Cheng SH, Liu JM, Liu QY, Luo DY, Liao BH, et al. (2014) Prognostic role of microvessel density in patients with renal cell carcinoma: A meta-analysis. Int J Clin Exp Pathol 7: 5855-5863.

41. Nawaz MI, Van Raemdonck K, Mohammad G, Kangave D, Van Damme J, et al. (2013) Autocrine CCL2, CXCL4, CXCL9 and CXCL10 signal in retinal endothelial cells and are enhanced in diabetic retinopathy. Exp Eye Res 109: 67-76.

42. Oh IY, Yoon CH, Hur J, Kim JH, Kim TY, et al. (2007) Involvement of E-selectin in recruitment of endothelial progenitor cells and angiogenesis in ischemic muscle. Blood 110: 3891-3899.

43. Xia W, de Bock C, Murrell GA, Wang Y (2003) Expression of urokinase-type plasminogen activator and its receptor is up-regulated during tendon healing. J Orthop Res 21: 819-825.

44. Baj A, Beltramini GA, Romano M, Lauritano D, Gaudio RM, et al. (2017) Genetic effects of BIOPAD® on fibroblast primary culture. J Biol Regul Homeost Agents 31: 209-214.

45. Davies MR, Lee L, Feeley BT, Kim HT, Liu X (2017) Lysophosphatidic acid-induced RhoA signaling and prolonged macrophage infiltration worsens fibrosis and fatty infiltration following rotator cuff tears. J Orthop Res 35: 1539-1547.

46. Guarda G, Dostert C, Staehli F, Cabalzar K, Castillo R, et al. (2009) T cells dampen innate immune responses through inhibition of NLRP1 and NLRP3 inflammasomes. Nature 460: 269-273.

47. Canton J (2014) Phagosome maturation in polarized macrophages. J Leukoc Biol 96: 729-738.

48. Michalski MN, LK McCauley (2017) Macrophages and skeletal health. Pharmacol Ther 174: 43-54.

49. Delgado-Bellido D, Serrano-Saenz S, Fernández-Cortés M, Oliver FJ (2017) Vasculogenic mimicry signaling revisited: focus on non-vascular VE-cadherin. Mol Cancer 16: 65.

50. Dean BJ, AJ Carr (2016) The Effects of Glucocorticoid on Tendon and Tendon Derived Cells. Adv Exp Med Biol 920: 239-246.

51. Heinemeier KM, Øhlenschlæger TF, Mikkelsen UR, Sønder F, Schjerling P, et al. (2017) Effects of anti-inflammatory (NSAID) treatment on human tendinopathic tissue. J Appl Physiol 123: 1397-1405.

52. Pingel J, Fredberg U, Mikkelsen LR, Schjerling P, Heinemeier KM, et al. (2013) No inflammatory gene-expression response to acute exercise in human Achilles tendinopathy. Eur J Appl Physiol 113: 2101-2109.

53. Plaas A, Sandy JD, Liu H, Diaz MA, Schenkman D, et al. (2011) Biochemical identification and immunolocalizaton of aggrecan, ADAMTS5 and inter-alpha-trypsin-inhibitor in equine degenerative suspensory ligament desmitis. J Orthop Res 29: 900-906.

54. Cook JL, Purdam CR (2009) Is tendon pathology a continuum? A pathology model to explain the clinical presentation of load-induced tendinopathy. Br J Sports Med 43: 409-416.

55. Cook JL, Rio E, Purdam CR, Docking SI (2016) Revisiting the continuum model of tendon pathology: What is its merit in clinical practice and research? Br J Sports Med 50: 1187-1191.

Supplementary Table 1: Experimental Groups and Replicates assayed for outcome measures.

Experimental group	Histology/IHC[2]	qt-PCR Arrays[3]	Biomechanics[4]
Un-Injured (UI)[1]	N = 3	N = 3 (16,16,20)	N = 8
3 days (3 d)	N = 3	N = 2 (14,16)	not determined
9 days (9 d)	N = 3	N = 2 (16,16)	not determined
25 days (25 d)	N = 3	N = 3 (16,16,18)	N = 9
Oral IBU 3-25 days (E-IBU)	N = 3	N = 3 (16,16,18)	N = 11
Oral IBU 9-25 days (L-IBU)	N = 3	N = 3 (14,16,18)	N = 11
Oral IBU 3-25 days (UI-IBU)	N = 3	N = 2 (16,18)	N = 9
Number of Mice	21	238	48

[1]UI for Histology and qPCR 12-week-old mice; UI for Biomechanics 16-week-old mice; [2]Individual legs;
[3]Replicate Tissue pools with number of tendons per pool in parenthesis; [4]Individual Tendons.

Supplementary Table 2: Wound healing gene arrays.

Mm.213025	Acta2	Actin, alpha 2, smooth muscle, aorta
Mm.686	Actc1	Actin, alpha, cardiac muscle 1
Mm.309336	Angpt1	Angiopoietin 1
Mm.867	Ccl12	Chemokine (C-C motif) ligand 12
Mm.341574	Ccl7	Chemokine (C-C motif) ligand 7
Mm.4861	Cd40lg	CD40 ligand
Mm.35605	Cdh1	Cadherin 1
Mm.297859	Col14a1	Collagen, type XIV, alpha 1
Mm.277735	Col1a1	Collagen, type I, alpha 1
Mm.277792	Col1a2	Collagen, type I, alpha 2
Mm.249555	Col3a1	Collagen, type III, alpha 1
Mm.738	Col4a1	Collagen, type IV, alpha 1
Mm.389135	Col4a3	Collagen, type IV, alpha 3
Mm.7281	Col5a1	Collagen, type V, alpha 1
Mm.10299	Col5a2	Collagen, type V, alpha 2
Mm.334994	Col5a3	Collagen, type V, alpha 3
Mm.4922	Csf2	Colony stimulating factor 2 (granulocyte-macrophage)
Mm.1238	Csf3	Colony stimulating factor 3 (granulocyte)
Mm.390287	Ctgf	Connective tissue growth factor
Mm.291928	Ctnnb1	Catenin (cadherin associated protein), beta 1
Mm.4858	Ctsg	Cathepsin G
Mm.272085	Ctsk	Cathepsin K
Mm.9304	Ctsl	Cathepsin L
Mm.21013	Cxcl1	Chemokine (C-X-C motif) ligand 1
Mm.131723	Cxcl11	Chemokine (C-X-C motif) ligand 11
Mm.244289	Cxcl3	Chemokine (C-X-C motif) ligand 3
Mm.4660	Cxcl5	Chemokine (C-X-C motif) ligand 5
Mm.252481	Egf	Epidermal growth factor
Mm.8534	Egfr	Epidermal growth factor receptor
Mm.235105	F13a1	Coagulation factor XIII, A1 subunit
Mm.273188	F3	Coagulation factor III
Mm.88793	Fga	Fibrinogen alpha chain
Mm.317323	Fgf10	Fibroblast growth factor 10
Mm.473689	Fgf2	Fibroblast growth factor 2
Mm.330557	Fgf7	Fibroblast growth factor 7
Mm.289681	Hbegf	Heparin-binding EGF-like growth factor
Mm.267078	Hgf	Hepatocyte growth factor
Mm.240327	Ifng	Interferon gamma
Mm.268521	Igf1	Insulin-like growth factor 1
Mm.874	Il10	Interleukin 10
Mm.222830	Il1b	Interleukin 1 beta
Mm.14190	Il2	Interleukin 2
Mm.276360	Il4	Interleukin 4
Mm.1019	Il6	Interleukin 6
Mm.4364	Il6st	Interleukin 6 signal transducer
Mm.482186	Itga1	Integrin alpha 1
Mm.5007	Itga2	Integrin alpha 2
Mm.57035	Itga3	Integrin alpha 3
Mm.31903	Itga4	Integrin alpha 4
Mm.16234	Itga5	Integrin alpha 5 (fibronectin receptor alpha)
Mm.225096	Itga6	Integrin alpha 6
Mm.2272	Itgav	Integrin alpha V
Mm.263396	Itgb1	Integrin beta 1 (fibronectin receptor beta)
Mm.87150	Itgb3	Integrin beta 3
Mm.6424	Itgb5	Integrin beta 5
Mm.98193	Itgb6	Integrin beta 6
Mm.196581	Mapk1	Mitogen-activated protein kinase 1
Mm.8385	Mapk3	Mitogen-activated protein kinase 3
Mm.2326	Mif	Macrophage migration inhibitory factor
Mm.156952	Mmp1a	Matrix metallopeptidase 1a (interstitial collagenase)
Mm.29564	Mmp2	Matrix metallopeptidase 2
Mm.4825	Mmp7	Matrix metallopeptidase 7
Mm.4406	Mmp9	Matrix metallopeptidase 9
Mm.2675	Pdgfa	Platelet derived growth factor, alpha
Mm.154660	Plat	Plasminogen activator, tissue
Mm.4183	Plau	Plasminogen activator, urokinase
Mm.1359	Plaur	Plasminogen activator, urokinase receptor
Mm.971	Plg	Plasminogen
Mm.245395	Pten	Phosphatase and tensin homolog
Mm.292547	Ptgs2	Prostaglandin-endoperoxide synthase 2
Mm.292510	Rac1	RAS-related C3 botulinum substrate 1
Mm.757	Rhoa	Ras homolog gene family, member A
Mm.250422	Serpine1	Serine (or cysteine) peptidase inhibitor, clade E, member 1
Mm.249934	Stat3	Signal transducer and activator of transcription 3
Mm.283283	Tagln	Transgelin
Mm.137222	Tgfa	Transforming growth factor alpha
Mm.248380	Tgfb1	Transforming growth factor, beta 1
Mm.200775	Tgfbr3	Transforming growth factor, beta receptor III
Mm.8245	Timp1	Tissue inhibitor of metalloproteinase 1
Mm.1293	Tnf	Tumor necrosis factor
Mm.282184	Vegfa	Vascular endothelial growth factor A
Mm.3667	Vtn	Vitronectin
Mm.10222	Wisp1	WNT1 inducible signaling pathway protein 1
Mm.287544	Wnt5a	Wingless-related MMTV integration site 5A

Mm.328431	Actb	Actin, beta
Mm.163	B2m	Beta-2 microglobulin
Mm.343110	Gapdh	Glyceraldehyde-3-phosphate dehydrogenase
Mm.3317	Gusb	Glucuronidase, beta
Mm.2180	Hsp90ab1	Heat shock protein 90 alpha (cytosolic), class B member 1

Supplementary Table 3: NFκb target genes array.

Mm.1408	Adm	Adrenomedullin
Mm.301626	Agt	Angiotensinogen (serpin peptidase inhibitor, clade A, member)
Mm.6645	Akt1	Thymoma viral proto-oncogene 1
Mm.398221	Aldh3a2	Aldehyde dehydrogenase family 3, subfamily A2
Mm.425593	Bcl2a1a	B-cell leukemia/lymphoma 2 related protein A1a
Mm.238213	Bcl2l1	Bcl2-like 1
Mm.335659	Birc2	Baculoviral IAP repeat-containing 2
Mm.2026	Birc3	Baculoviral IAP repeat-containing 3
Mm.19131	C3	Complement component 3
Mm.477109	C4a	Complement component 4A (Rodgers blood group)
Mm.867	Ccl12	Chemokine (C-C motif) ligand 12
Mm.12895	Ccl22	Chemokine (C-C motif) ligand 22
Mm.284248	Ccl5	Chemokine (C-C motif) ligand 5
Mm.273049	Ccnd1	Cyclin D1
Mm.14302	Ccr5	Chemokine (C-C motif) receptor 5
Mm.271833	Cd40	CD40 antigen
Mm.439737	Cd74	CD74 antigen (invariant polypeptide of major histocompatibility complex)
Mm.89474	Cd80	CD80 antigen
Mm.57175	Cd83	CD83 antigen
Mm.195663	Cdkn1a	Cyclin-dependent kinase inhibitor 1A (P21)
Mm.653	Cfb	Complement factor B
Mm.795	Csf1	Colony stimulating factor 1 (macrophage)
Mm.4922	Csf2	Colony stimulating factor 2 (granulocyte-macrophage)
Mm.235324	Csf2rb	Colony stimulating factor 2 receptor, beta, low-affinity (granulocyte-macrophage)
Mm.1238	Csf3	Colony stimulating factor 3 (granulocyte)
Mm.21013	Cxcl1	Chemokine (C-X-C motif) ligand 1
Mm.877	Cxcl10	Chemokine (C-X-C motif) ligand 10
Mm.244289	Cxcl3	Chemokine (C-X-C motif) ligand 3
Mm.766	Cxcl9	Chemokine (C-X-C motif) ligand 9
Mm.8534	Egfr	Epidermal growth factor receptor
Mm.290421	Egr2	Early growth response 2
Mm.273188	F3	Coagulation factor III
Mm.1805	F8	Coagulation factor VIII
Mm.1626	Fas	Fas (TNF receptor superfamily member 6)
Mm.3355	Fasl	Fas ligand (TNF superfamily, member 6)
Mm.1360	Gadd45b	Growth arrest and DNA-damage-inducible 45 beta
Mm.435508	Icam1	Intercellular adhesion molecule 1
Mm.1245	Ifnb1	Interferon beta 1, fibroblast
Mm.240327	Ifng	Interferon gamma
Mm.239707	Il12b	Interleukin 12B
Mm.4392	Il15	Interleukin 15
Mm.15534	Il1a	Interleukin 1 alpha
Mm.222830	Il1b	Interleukin 1 beta
Mm.1349	Il1r2	Interleukin 1 receptor, type II
Mm.8827	Il1rn	Interleukin 1 receptor antagonist
Mm.14190	Il2	Interleukin 2
Mm.915	Il2ra	Interleukin 2 receptor, alpha chain
Mm.276360	Il4	Interleukin 4
Mm.1019	Il6	Interleukin 6
Mm.4946	Ins2	Insulin II
Mm.105218	Irf1	Interferon regulatory factor 1
Mm.87787	Lta	Lymphotoxin A
Mm.1715	Ltb	Lymphotoxin B
Mm.14487	Map2k6	Mitogen-activated protein kinase kinase
Mm.333284	Mitf	Microphthalmia-associated transcription factor
Mm.4406	Mmp9	Matrix metallopeptidase 9
Mm.2444	Myc	Myelocytomatosis oncogene
Mm.213003	Myd88	Myeloid differentiation primary response gene 88
Mm.476883	Ncoa3	Nuclear receptor coactivator 3
Mm.256765	Nfkb1	Nuclear factor of kappa light polypeptide gene enhancer in B-cells 1, p105
Mm.102365	Nfkb2	Nuclear factor of kappa light polypeptide gene enhancer in B-cells 2, p49/p100
Mm.170515	Nfkbia	Nuclear factor of kappa light polypeptide gene enhancer in B-cells inhibitor, alpha
Mm.252	Nqo1	NAD(P)H dehydrogenase, quinone 1
Mm.3507	Nr4a2	Nuclear receptor subfamily 4, group A, member 2
Mm.144089	Pdgfb	Platelet derived growth factor, B polypeptide
Mm.4183	Plau	Plasminogen activator, urokinase
Mm.292547	Ptgs2	Prostaglandin-endoperoxide synthase 2
Mm.4869	Rel	Reticuloendotheliosis oncogene
Mm.249966	Rela	V-rel reticuloendotheliosis viral oncogene homolog A (avian)
Mm.1741	Relb	Avian reticuloendotheliosis viral (v-rel) oncogene related B
Mm.5245	Sele	Selectin, endothelial cell
Mm.3337	Selp	Selectin, platelet
Mm.45953	Snap25	Synaptosomal-associated protein 25
Mm.290876	Sod2	Superoxide dismutase 2, mitochondrial
Mm.277406	Stat1	Signal transducer and activator of transcription 1
Mm.249934	Stat3	Signal transducer and activator of transcription 3
Mm.34064	Stat5b	Signal transducer and activator of transcription 5B
Mm.1293	Tnf	Tumor necrosis factor
Mm.235328	Tnfrsf1b	Tumor necrosis factor receptor superfamily, member 1b
Mm.1062	Tnfsf10	Tumor necrosis factor (ligand) superfamily, member 10
Mm.3399	Traf2	Tnf receptor-associated factor 2
Mm.222	Trp53	Transformation related protein 53
Mm.76649	Vcam1	Vascular cell adhesion molecule 1
Mm.259879	Xiap	X-linked inhibitor of apoptosis

Mm.328431	Actb	Actin, beta
Mm.163	B2m	Beta-2 microglobulin
Mm.343110	Gapdh	Glyceraldehyde-3-phosphate dehydrogenase
Mm.3317	Gusb	Glucuronidase, beta
Mm.2180	Hsp90ab1	Heat shock protein 90 alpha (cytosolic), class B member 1

Supplementary Table 4: Mean mRNA Abundance of individual genes in UI pools (ND* = Not detectable, ΔCt > 14.0).

Wound healing	n = 3 pools	Nfκb Targets	n = 3 pools
Acta2	362	*Adm*	5
Actc1	43	*Agt*	4.9
Angpt1	25	*Akt1*	81.8
Ccl12	13.8	*Aldh3a2*	35
Ccl7	18	*Bcl2a1a*	1.5
Cd40lg	0.2	*Bcl2l1*	40.4
Cdh1	0.1	*Birc2*	44.8
Col14a1	35	*Birc3*	14.9
Col1a1	4219	*C3*	230.2
Col1a2	11944.7	*C4a*	0.2
Col3a1	5239.6	*Ccl12*	13
Col4a1	101.3	*Ccl22*	0.8
Col4a3	0.7	*Ccl5*	2.3
Col5a1	183.2	*Ccnd1*	58.9
Col5a2	421.9	*Ccr5*	6.7
Col5a3	113	*Cd40*	3.5
Csf2	0.1	*Cd74*	563.8
Csf3	0.5	*Cd80*	5.4
Ctgf	1315.3	*Cd83*	4
Ctnnb1	137.5	*Cdkn1a*	89.2
Ctsg	0.1	*Cfb*	135.9
Ctsk	209.1	*Csf1*	77.4
Ctsl	430.7	*Csf2*	ND*
Cxcl1	0.3	*Csf2rb*	18.3
Cxcl11	1.5	*Csf3*	ND*
Cxcl3	0.2	*Cxcl1*	0.2
Cxcl5	0.2	*Cxcl10*	1.9
Egf	1.8	*Cxcl3*	0.1
Egfr	53.6	*Cxcl9*	0.4
F13a1	138.7	*Egfr*	84.4
F3	41.2	*Egr2*	4
Fga	ND*	*F3*	47.7
Fgf10	12.4	*F8*	0.6
Fgf2	25.9	*Fas*	49.4
Fgf7	29.4	*Fasl*	ND*
Hbegf	29.3	*Gadd45b*	22.6
Hgf	1.6	*Icam1*	18.3
Ifng	ND*	*Ifnb1*	ND*
Igf1	75.5	*Ifng*	ND*
Il10	0.3	*Il12b*	0.1
Il1b	0.7	*Il15*	12.1
Il2	ND*	*Il1a*	0.5
Il4	0.4	*Il1b*	0.7
Il6	0.3	*Il1r2*	2
Il6st	332.8	*Il1rn*	0.5
Itga1	43.7	*Il2*	ND*
Itga2	18.1	*Il2ra*	2.6
Itga3	3	*Il4*	1.1
Itga4	2.6	*Il6*	0.1
Itga5	34.2	*Ins2*	ND*
Itga6	46.7	*Irf1*	15.9
Itgav	66.3	*Lta*	0.2
Itgb1	361.2	*Ltb*	1.3
Itgb3	9	*Map2k6*	12.4
Itgb5	285.7	*Mitf*	47.4
Itgb6	12.6	*Mmp9*	3.8
Mapk1	107.5	*Myc*	19.9
Mapk3	37.9	*Myd88*	1.9
Mif	130.5	*Ncoa3*	30.1
Mmp1a	ND*	*Nfkb1*	61.9
Mmp2	459.4	*Nfkb2*	4.4
Mmp7	ND*	*Nfkbia*	139.4
Mmp9	1.5	*Nqo1*	27
Pdgfa	24.2	*Nr4a2*	10
Plat	20.1	*Pdgfb*	25.8
Plau	19	*Plau*	18.6
Plaur	7	*Ptgs2*	0.6
Plg	0.2	*Rel*	6.8
Pten	165.1	*Rela*	17.8
Ptgs2	0.8	*Relb*	1.4
Rac1	346.4	*Sele*	4.2
Rhoa	413.9	*Selp*	17.2
Serpine1	1.5	*Snap25*	ND*
Stat3	14.3	*Sod2*	150.6
Tagln	172	*Stat1*	30.1
Tgfa	0.7	*Stat3*	108.9
Tgfb1	69.8	*Stat5b*	35.2
Tgfbr3	151.5	*Tnf*	1.6
Timp1	0.1	*Tnfrsf1b*	19.5
Tnf	0.5	*Tnfsf10*	11.6
Vegfa	53.5	*Traf2*	12.2
Vtn	16.8	*Trp53*	14.2
Wisp1	12.4	*Vcam1*	5.2
Wnt5a	6.6	*Xiap*	30.2

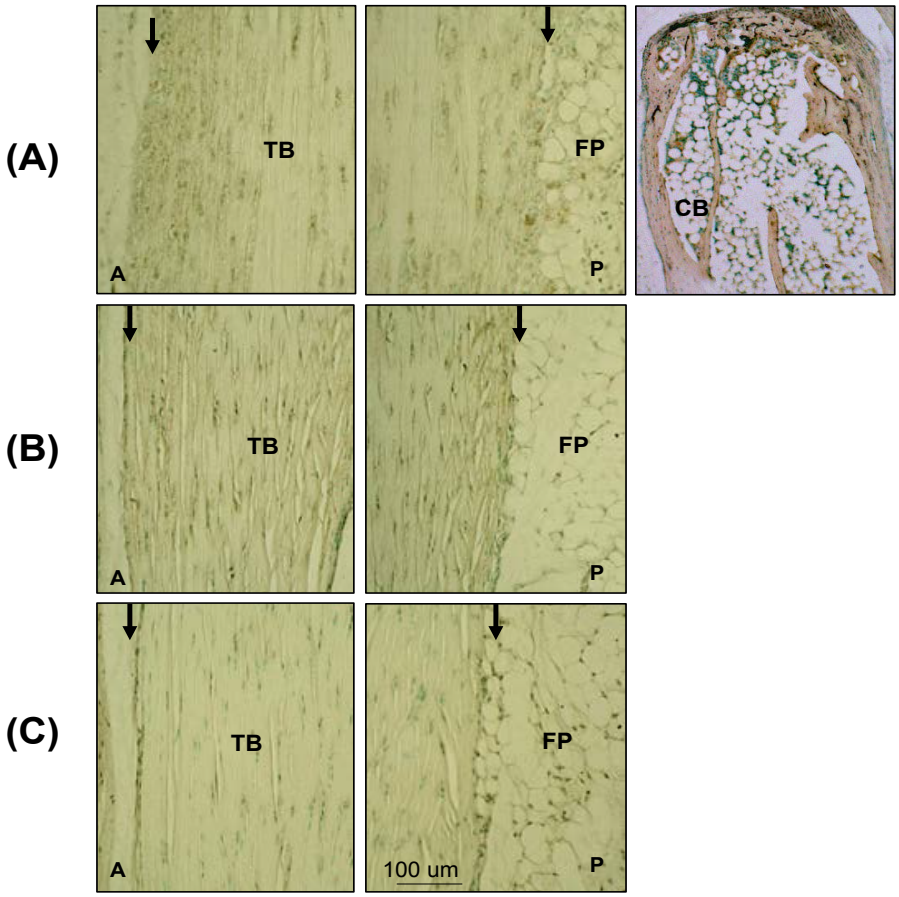

Supplementary Figure 1: Negative control Images for IHC and Immunochemistry.

Sections were treated (A) with non-immune rabbit serum, following Proteinase K treatment, (B) without GSI Lectin or (C) biotinylated HABP following Streptomyces Hyaluronidase digestion of HA. TB: Tendon Body; FP: Fat Pad; P: Posterior; CB: Calcaneus Bone; A: Anterior; Peritenon regions are indicated by black arrows. The staining of the cancellous bone represents non-specific staining due to binding of the secondary antibody in proteinase K pretreated samples.

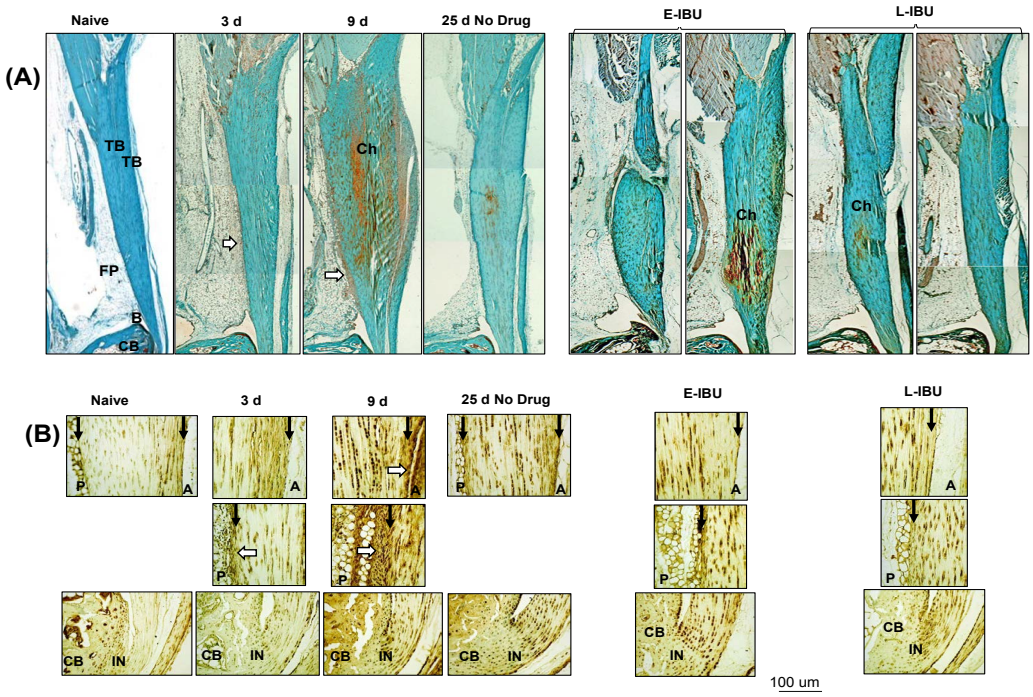

Supplementary Figure 2: SafO staining (A) and Aggrecan IHC (B) of the Achilles tendon and surrounding tissues, pre- and post-injury and after IBU dosing.

Sagittal sections were stained as described in the Methods. TB: Tendon Body; FP: Fat Pad; B: Bursa; CB: Cancellous Bone; Ch: Chondroid; P: Posterior; A: Anterior; IN: Insertion site. Areas of increased cellularity of the periosteum and adipose stroma are indicated by white arrows. Anterior and Posterior peritenon regions are indicated by black arrows.

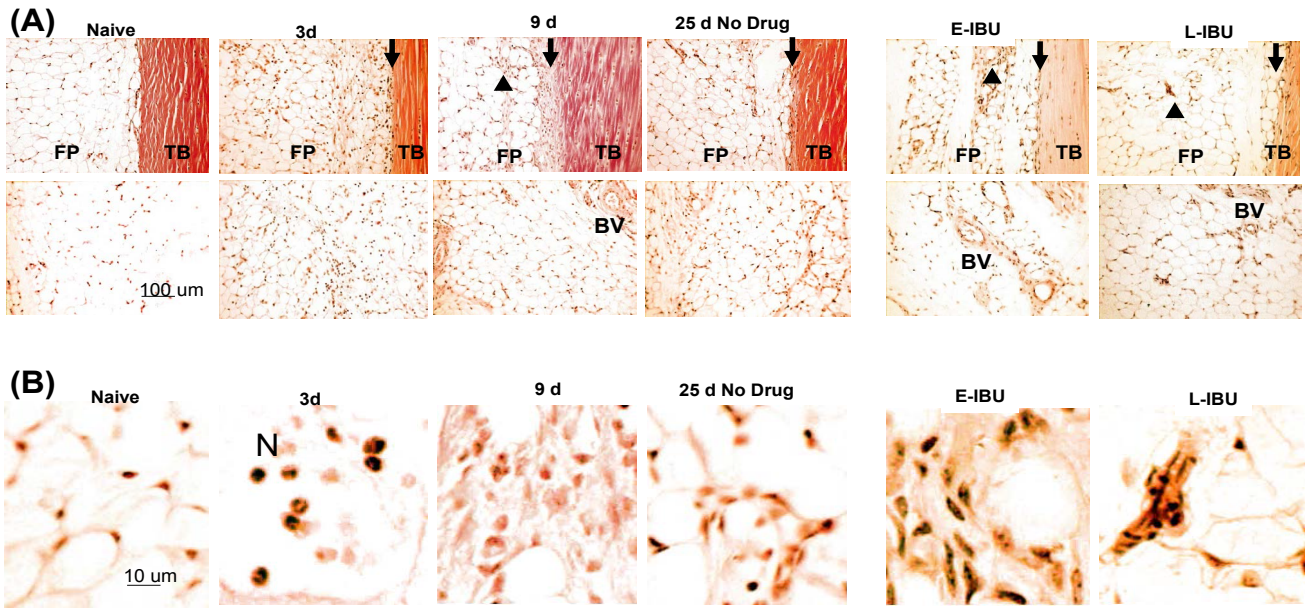

Supplementary Figure 3: Altered cellularity in posterior Peritenon and fat pad following injury and after IBU treatment.

Panel A : Sagittal sections were stained as described in the Methods. TB: Tendon Body; FP: Fat Pad; N: Neutrophils; BV: Blood vessel; black arrows show the peritenon regions. Accumulation of neutrophils in the fat pad stroma in 3 d samples, hyperproliferated stromal cells at 9 d and persistent accumulation of hypercellularity in the adipose stroma after IBU treatment are marked by black arrow heads. A high magnification of these cells is shown in panel B.

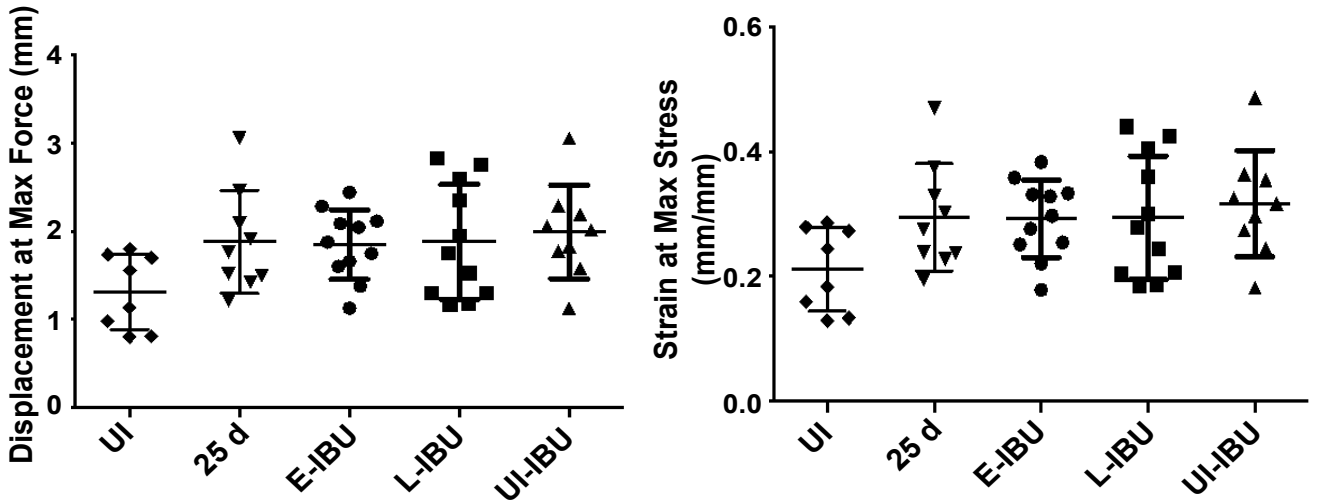

Supplementary Figure 4: Effect of IBU administration on Achilles tendon mechanical properties.

The scatter plots show data for individual tendons in each group. For each group, horizontal lines denote mean ± one standard deviation.